



A Crack Identification Method For Beam Type Structures Subject To Moving Vehicle Using Particle Swarm Optimization

Hakan GÖKDAĞ^{1,*}

¹*Bursa Technical University Natural Sciences, Architecture and Engineering Faculty Mechanical Engineering Department, 16190 Osmangazi, Bursa, Turkey*

Received: 17.04.2012 Accepted: 15.03.2013

ABSTRACT

In this work a crack identification method for beam type structures under moving vehicle is proposed. The basic of the method is to formulate damage detection as an inverse problem, and solve for damage locations and extents. To this end, an objective function is defined based on the difference of damaged beam dynamic response and the response calculated by the mathematical model of the beam. The optimization problem is solved through a popular evolutionary algorithm, i.e. the particle swarm optimization (PSO) with constriction factor, to obtain crack locations and depths. From the numerical simulations it was observed that cracks with depth ratio of 0.1 can be identified with reasonable error by the present method in spite of noise interference and distortive effect of road surface roughness.

Key Words: Cracked beam, damage detection, particle swarm optimization, moving vehicle

1. INTRODUCTION

Structures under moving load have many practical applications such as railway tracks, bridges, pipelines, roadways, etc. Since moving load yields larger deflections and higher stresses than equivalent static load conditions, dynamics of such structures has received considerable attention in the literature [1]. If the host structure has crack-like local defects, then the impact of moving load becomes more pronounced. In the earlier study on this issue Mahmoud [2] demonstrated that crack shifts the minimum point of deflection profile to the right-hand on the time axis. Bilello and Bergman [3] concluded that changes in the time-response of the beam due to damage are more perceptible in comparison to the changes in the natural

frequencies. Law and Zhu [4] investigated the effects of open and breathing cracks on the response of concrete bridges. Ariaei et al. [5] performed a similar study for beams with breathing cracks subject to moving mass. On the other hand, various damage detection methods have been developed for beams subject to moving load/vehicle using the continuous wavelet transform (CWT) [6-10]. They are based on the fact that CWT coefficients of beam dynamic response demonstrate local peaks at crack locations, and magnitudes of these peaks are proportional to crack depths.

In structural damage detection there are other methods based on model updating. The basic of these methods is to update mathematical or finite element model of the structure to match the calculated response to the one

*Corresponding author, e-mail: hakan.gokdag@btu.edu.tr

measured from damaged structure. This is achieved through an optimization procedure. To solve the optimization problem evolutionary methods are generally preferred, as they do not require gradient calculation, and have less possibility of being trapped by local minima in comparison with the gradient based methods [11-14]. One of these algorithms is the particle swarm optimization (PSO). PSO, developed by Kennedy and Eberhart [15], is a stochastic optimization technique inspired by natural flocking and swarm behavior of birds and insects. It is known to have less parameters and rapid convergence compared with the genetic algorithms (GA) [16], and has been successfully employed in model updating based damage detection applications [12-14]. In model updating based damage detection, time dependent structural response is used, as well. Buezas et al. [11] formulated an optimization problem using time responses from several points on the beam, and determined crack size and depth by solving this problem.

In the present work, motivated by the conclusion of Bilello and Bergman [3] mentioned above and the method of Buezas et al. [11], a model update based damage detection approach has been proposed for

bridge type structures carrying moving vehicle. In this respect, time dependent deflections from several points on a cracked beam were obtained, and an objective function was defined by subtracting these from the ones calculated by the mathematical model of the structure. Then, the PSO is employed to minimize this objective function to determine crack locations and depths. To the best of the author's knowledge, this is the first published study which deals with formulating damage detection in a beam with rough surface and subject to moving vehicle as an inverse problem and solving by the PSO algorithm for crack identification.

2. MATERIAL AND METHOD

2.1. Dynamic Response of the Beam

Figure 1 illustrates the beam-vehicle system. The Euler-Bernoulli model is considered for the beam, and half car model is adopted for the vehicle moving with the speed V . An open crack with depth h_1 is located at z_1 on the beam. Surface unevenness of the beam is regarded and tyres are assumed to be always in contact with the beam. Under these assumptions the equations of motion for the vehicle and beam can be derived as follows:

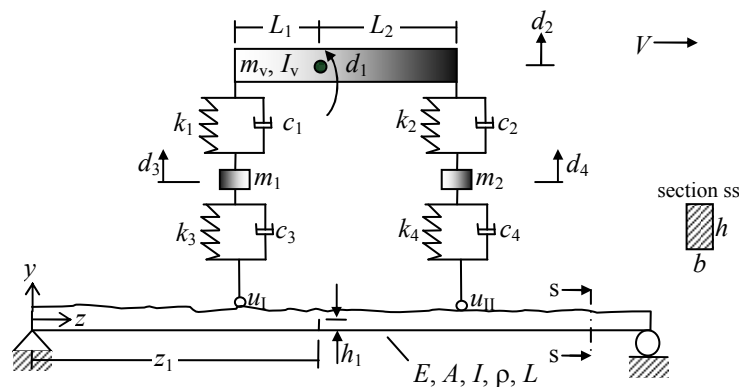


Figure 1. Beam-vehicle system.

$$\begin{bmatrix} I_v & 0 & 0 & 0 \\ 0 & m_v & 0 & 0 \\ 0 & 0 & m_1 & 0 \\ 0 & 0 & 0 & m_2 \end{bmatrix} \begin{Bmatrix} \ddot{d}_1 \\ \ddot{d}_2 \\ \ddot{d}_3 \\ \ddot{d}_4 \end{Bmatrix} + \begin{bmatrix} c_1 L_1^2 + c_2 L_2^2 & L_2 c_2 - L_1 c_1 & L_1 c_1 & -L_2 c_2 \\ L_2 c_2 - L_1 c_1 & c_2 + c_1 & -c_1 & -c_2 \\ L_1 c_1 & -c_1 & c_3 + c_1 & 0 \\ -L_2 c_2 & -c_2 & 0 & c_2 + c_4 \end{bmatrix} \begin{Bmatrix} \dot{d}_1 \\ \dot{d}_2 \\ \dot{d}_3 \\ \dot{d}_4 \end{Bmatrix} + \begin{bmatrix} k_1 L_1^2 + k_2 L_2^2 & L_2 k_2 - L_1 k_1 & L_1 k_1 & -L_2 k_2 \\ L_2 k_2 - L_1 k_1 & k_2 + k_1 & -k_1 & -k_2 \\ L_1 k_1 & -k_1 & k_3 + k_1 & 0 \\ -L_2 k_2 & -k_2 & 0 & k_2 + k_4 \end{bmatrix} \begin{Bmatrix} d_1 \\ d_2 \\ d_3 \\ d_4 \end{Bmatrix} = \begin{Bmatrix} 0 \\ 0 \\ k_3 \delta_I(u+r) + c_3 \delta_I(\dot{u} + r'V) \\ k_4 \delta_{II}(u+r) + c_4 \delta_{II}(\dot{u} + r'V) \end{Bmatrix} \tag{1}$$

$$\rho A \frac{\partial^2 y(z,t)}{\partial t^2} + C \frac{\partial y(z,t)}{\partial t} + EI \frac{\partial^4 y(z,t)}{\partial x^4} = -P_I \delta_I - P_{II} \delta_{II} \tag{2}$$

where $L_v, m_v, m_1, m_2, L_1, L_2, k_1, k_2, k_3, c_1, c_2, c_3, c_4$ are vehicle parameters shown in Fig.1, C is the damping of beam material. $d_i, i=1:4$, denote vehicle degrees of freedom, δ_I and δ_{II} are the Dirac delta functions

defined as $\delta_I = \delta(z - Vt - (L_1 + L_2))$, $\delta_{II} = \delta(z - Vt)$. P_I and P_{II} are the interaction forces acting on the beam through the contact points I and II, as follows:

$$P_I = \left(m_1 + \frac{L_2}{L_1 + L_2} m_v \right) 9.81 + k_3(u + r - d_3) + c_3(\dot{u} + r'V - \dot{d}_3) \tag{3a}$$

$$P_{II} = \left(m_2 + \frac{L_1}{L_1 + L_2} m_v \right) 9.81 + k_4(u + r - d_4) + c_4(\dot{u} + r'V - \dot{d}_4) \tag{3b}$$

where u is the vertical displacement at the tyre contact point, i.e. $u = y(z, t)$, its derivative with respect to time is

$\dot{u} = d(y(z, t))/dt = V \partial y(z, t) / \partial z + \partial y(z, t) / \partial t$, and $r' = d / dz$. Road surface roughness function in Eq. (3) is [17]

$$r(z) = \sum_{k=1}^N \left[\left(4S_d(f_0) \left(\frac{2\pi k}{L_c f_0} \right)^{-2} \frac{2\pi}{L_c} \right)^{1/2} \cos \left(\frac{2\pi k f_0}{L_c} z + \theta_k \right) \right] \tag{4}$$

where $S_d(f_0)$ is the roughness coefficient in $m^3/cycles$, f_0 is the discontinuity frequency equal to $1/2\pi$ (cycle/m), L_c is twice the length of the beam, and θ_k is the uniform random number between 0 and 2π . $N=10^4$ is adopted in this study. The road classification according to the ISO standard is based on the value of roughness coefficient. Five classes representing different qualities of the road are A: very good, B: good, C: average, D:poor, E: very poor with the

roughness coefficients equal to 1×10^{-6} , 6×10^{-6} , 16×10^{-6} , 64×10^{-6} , 256×10^{-6} , respectively.

Assuming mode superposition, i.e. $y(z, t) = \mathbf{Y}(z)^T \mathbf{q}(t)$, substituting into Eq.(2), multiplying by $\mathbf{Y}(z)$ and integrating from 0 to L , and finally combining with Eq.(1) lead to the following coupled beam-vehicle equations:

$$\begin{bmatrix} \mathbf{M}_{N_m \times N_m} & \mathbf{0}_{N_m \times 4} \\ \mathbf{0}_{4 \times N_m} & \bar{\mathbf{M}}_{4 \times 4} \end{bmatrix} \begin{Bmatrix} \dot{\mathbf{q}} \\ \dot{\mathbf{d}} \end{Bmatrix} + \begin{bmatrix} \mathbf{C} + \bar{\mathbf{A}}_8 & \bar{\mathbf{A}}_{10} \\ -\mathbf{A}_6 & \bar{\mathbf{C}} \end{bmatrix} \begin{Bmatrix} \mathbf{q} \\ \mathbf{d} \end{Bmatrix} + \begin{bmatrix} \mathbf{K} + \bar{\mathbf{A}}_7 & \bar{\mathbf{A}}_9 \\ -\mathbf{A}_5 & \bar{\mathbf{K}} \end{bmatrix} \begin{Bmatrix} \mathbf{q} \\ \mathbf{d} \end{Bmatrix} = \begin{Bmatrix} \mathbf{F}_1 \\ \mathbf{F}_2 \end{Bmatrix} \tag{5}$$

where $\mathbf{M} = \int_0^L \rho A \mathbf{Y} \mathbf{Y}^T dz$, $\mathbf{C} = \int_0^L C \mathbf{Y} \mathbf{Y}^T dz$, $\mathbf{K} = \int_0^L E I \mathbf{Y} \mathbf{Y}^T dz$. $\bar{\mathbf{M}}, \bar{\mathbf{C}}, \bar{\mathbf{K}}$ are the mass, damping and stiffness matrices in Eq.(1), N_m is the number of modes used, $\mathbf{Y}(z)$ is the vector of size $N_m \times 1$ containing vibration modes of the cracked beam, and $\mathbf{q}(t)$ stands for the modal coordinates. Additionally,

$$\mathbf{A}_1 = [\mathbf{Y}(z)^T k_3 + V c_3 \mathbf{Y}'(z)^T] \delta_I, \mathbf{A}_2 = [\mathbf{Y}(z)^T c_3] \delta_I \tag{6a}$$

$$\mathbf{A}_3 = [\mathbf{Y}(z)^T k_4 + V c_4 \mathbf{Y}'(z)^T] \delta_{II}, \mathbf{A}_4 = [\mathbf{Y}(z)^T c_4] \delta_{II} \tag{6b}$$

$$\mathbf{A}_5 = \begin{bmatrix} \mathbf{0}_{2 \times N_m} \\ \mathbf{A}_1 \\ \mathbf{A}_2 \end{bmatrix}, \mathbf{A}_6 = \begin{bmatrix} \mathbf{0}_{2 \times N_m} \\ \mathbf{A}_2 \\ \mathbf{A}_4 \end{bmatrix}, \bar{\mathbf{A}}_j = \int_0^L \mathbf{Y}(z) \mathbf{A}_j dz, \tag{6c}$$

$j=7,8,9,10$

$$\begin{aligned} \mathbf{A}_7 &= \mathbf{A}_1 + \mathbf{A}_3, \mathbf{A}_8 = \mathbf{A}_2 + \mathbf{A}_4, \\ \mathbf{A}_9 &= [0 \quad 0 \quad -k_3 \quad -k_4], \\ \mathbf{A}_{10} &= [0 \quad 0 \quad -c_3 \quad -c_4] \end{aligned} \tag{6d}$$

$$\mathbf{F}_1 = \int_0^L \mathbf{Y}(z) ([W_1 + r k_3 + r' V c_3] \delta_I + [W_2 + r k_4 + r' V c_4] \delta_{II}) dz \tag{6e}$$

$$W_I = \left(m_1 + \frac{L_2}{L_1 + L_2} m_v \right) 9.81, \tag{6f}$$

$$W_{II} = \left(m_2 + \frac{L_1}{L_1 + L_2} m_v \right) 9.81$$

$$\mathbf{F}_2 = [0 \quad 0 \quad (r k_3 + r' V c_3) \delta_I \quad (r k_4 + r' V c_4) \delta_{II}]^T \tag{6g}$$

Eq.(5) can be solved by any numerical integration method. In this study Newmark- β method (with $\beta=1/6$ and $\gamma=1/2$ [18]) is employed for this purpose. Before solving the equation, vibration modes of the cracked

beam is required to obtain the coefficient matrices in Eq. (5). Assuming the beam is composed of two parts joined at the crack location through a rotational spring, we can write the following compatibility equations at the crack location [2]:

$$\begin{aligned} Y_1(z_1) &= Y_2(z_1), \quad Y'_1(z_1) + \theta Y''_1(z_1) = Y'_2(z_1), \\ Y''_1(z_1) &= Y''_2(z_1), \quad Y'''_1(z_1) = Y'''_2(z_1) \end{aligned} \quad (7)$$

Here $Y_i(z)$ is the mode shape of the i th beam part defined as follows

$$\theta = 2h \left(\frac{\bar{h}_1}{1-\bar{h}_1} \right)^2 \left(5.93 - 19.69\bar{h}_1 + 37.14\bar{h}_1^2 - 35.84\bar{h}_1^3 + 13.12\bar{h}_1^4 \right), \quad \bar{h}_1 = h_1/h \quad (9)$$

The eigenvalue problem is formulated using Eq.(7) along with the boundary conditions for the simple supports. Note that in the case of multiple cracks the number of Eq. (8) is equal to the number of cracks. Natural frequencies and vibration modes of the cracked beam can be obtained by solving the eigenvalue problem (see [2,5,6,10] for details). Using these vibration modes Eq.(5) is solved. Fig. 2 illustrates the normalized midspan deflection of the beam. The following numerical data for the beam-vehicle system are employed to obtain the figure [4]: $E = 210 \text{ GPa}$, $\rho = 7860 \text{ kgm}^{-3}$, $L = 30\text{m}$, $b = 0.4245\text{m}$, $h = 1.4986\text{m}$, $m_v = 17735 \text{ kg}$, $m_1 = 1000 \text{ kg}$, $m_2 = 1500 \text{ kg}$, $I_v = 1.47 \times 10^5 \text{ kgm}^2$, $k_1 = 4.23 \times 10^6 \text{ Nm}^{-1}$, $k_2 = 2.47 \times 10^6 \text{ Nm}^{-1}$, $k_3 = 4.6 \times 10^6 \text{ Nm}^{-1}$, $k_4 = 3.74 \times 10^6 \text{ Nm}^{-1}$, $c_1 = 4 \times 10^4 \text{ Nsm}^{-1}$, $c_2 = 3 \times 10^4 \text{ Nsm}^{-1}$, $c_3 = 4.3 \times 10^3 \text{ Nsm}^{-1}$, $c_4 = 3.9 \times 10^3 \text{ Nsm}^{-1}$, $L_1 = 2.054 \text{ m}$, $L_2 = 2.216 \text{ m}$. Normalization is made by dividing to the midspan deflection of the simply-supported beam loaded by concentrated static force P acting on the midspan, i.e. $PL^3/(48EI)$ where $P = 9.81(m_v + m_1 + m_2)$. The first six vibration modes of the beam, for which the natural frequencies are 3.90, 15.61, 35.13, 62.44, 97.57 140.5 Hz, are employed. Two percent modal damping is considered for each mode [4]. The moving load speed is $V = 10\text{m/s}$. The sampling frequency of the simulation is 500 Hz which can capture the response of the first six vibration modes of the beam. The roughness coefficient is $S_d(f_0) = 6 \times 10^{-6}$ and damage locations are $\bar{z}_1 = z_1/L = 0.33$, $\bar{z}_2 = z_2/L = 0.67$ with equal crack depth $\bar{h}_1 = h_1/h = 0.2$, $\bar{h}_2 = h_2/h = 0.2$. From Fig. 2 it is seen that damage has significant impact on the maximum amplitude while roughness affects the variation of deflection with time.

2.2. The Objective Function and the Constrains

The aim is to correlate the response of the damaged beam to the one calculated by the mathematical model of the structure. To achieve this, it is proposed to adjust

$$\begin{aligned} Y_i(z) &= C_{i1} \cos(\lambda z) + C_{i2} \sin(\lambda z) + C_{i3} \cosh(\lambda z) \\ &+ C_{i4} \sinh(\lambda z), \quad i=1,2 \end{aligned} \quad (8)$$

where $\lambda = (\rho A \omega^2 / EI)^{0.25}$. λ and ω are eigenvalue and natural frequency parameters, respectively, and C_{ij} are the constants to be determined by solving the eigenvalue problem. The geometric factor of the crack, θ , is defined as follows [2,5]

crack sizes and locations by solving an optimization problem. The objective function of the problem is introduced as follows.

$$f(\mathbf{z}) = \sum_{n=1}^{N_{mp}} \int_0^T \frac{|y(z_n, t) - \bar{y}(z_n, t)|}{\max(|\bar{y}(z_n, t)|)} dt \quad (10)$$

where N_{mp} is the number of measurement points on the beam, z_n is the location of the n th measurement point on the beam, \bar{y} denotes the reference displacements measured from damaged beam, y stands for the corresponding displacements computed by the mathematical model of the structure. T is the total time for the vehicle to move across the beam. \mathbf{z} is the vector containing crack location and size parameters, i.e.

$$\mathbf{z} = \{ \bar{h}_1, \bar{h}_2, \dots, \bar{h}_{N_c}, \bar{z}_1, \bar{z}_2, \dots, \bar{z}_{N_c} \}, \quad \bar{h}_i = \frac{h_i}{h}, \quad \bar{z}_i = \frac{z_i}{L} \quad (11)$$

where N_c denotes the number of cracks. As to the measurement points, it is better to chose them close to the midpoint, since maximum deflection occurs at the beam midspan. Thus, four points [11] on the beam were determined as $\{0.3 \ 0.5 \ 0.6 \ 0.7\}L$, i.e. $N_{mp} = 4$ in Eq. (10). If the number of cracks (N_c) is more than one, then extra constraints other than lower and upper boundaries should be introduced for the optimization algorithm to make search in the feasible region. With these explanations in mind, the optimization problem can be formulated as follows

$$\begin{aligned} &\min f(\mathbf{z}) \\ &\text{subject to:} \\ &\bar{z}_i - \bar{z}_{i+1} < 0, \quad i = 1, 2, \dots, N_c - 1 \\ &0 < \bar{z}_j < 1, \quad 0 \leq \bar{h}_j < 1, \quad j = 1, 2, \dots, N_c \end{aligned} \quad (12)$$

Crack locations and depths can be determined by solving Eq.(12). In this work the PSO is employed for this purpose, and its details are given in the next section.

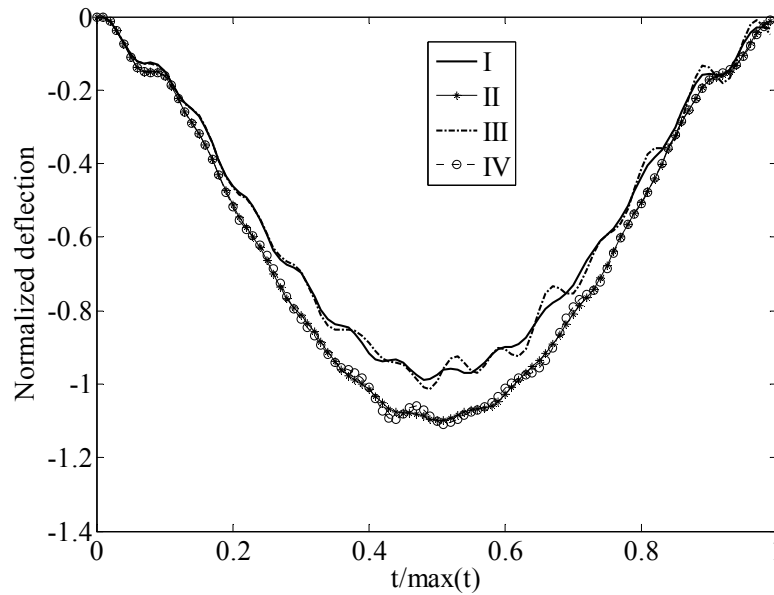


Figure 2. Normalized midspan deflections of the beam. I: damage (-), roughness (-), II: damage (+), roughness (-). III: damage (-), roughness (+), IV: damage (+), roughness (+). (-): not present, (+): present

2.3. The particle swarm optimization algorithm

PSO algorithm is initialized with a "swarm" composed of N particles. Particles refer to the candidate points in the search space of the optimization problem. To obtain the best solution each particle adjusts its trajectory toward its own previous best position and toward the previous best position of the swarm. By this way, each particle moves in the search space with an adaptive velocity, and stores the best position of the search space. Location (x) and velocity (v) of a particle are updated with the following equations [15,16].

$$\begin{aligned}
 v_{ij}^{k+1} &= v_{ij}^k + c_1 R_1 (p_{ij}^k - x_{ij}^k) + c_2 R_2 (p_{gj}^k - x_{ij}^k) \\
 x_{ij}^{k+1} &= x_{ij}^k + v_{ij}^{k+1}, \quad i = 1, 2, \dots, N, \\
 j &= 1, 2, \dots, m, \quad k = 1, 2, \dots, K_{\max}
 \end{aligned}
 \tag{13}$$

where k is the iteration counter, K_{\max} denotes the maximum number of iterations, m is the problem dimension, p_{ij}^k and p_{gj}^k are, respectively, the best positions of the i th particle and the swarm found until the k th iteration, R_1 and $R_2 \in U(0,1)$, where U means uniform random distribution, c_1 and c_2 are positive weighting constants called cognitive and social coefficients, respectively. These two constants regulate the relative velocity toward the global and local best points. The algorithm using Eq.(13) is called standard PSO. Clerc and Kennedy [19], introducing the constriction factor (χ), developed another version known as contemporary PSO (CPSO) [16], in which the velocity of each particle is updated as follows.

$$v_{ij}^{k+1} = \chi (v_{ij}^k + c_1 R_1 (p_{ij}^k - x_{ij}^k) + c_2 R_2 (p_{gj}^k - x_{ij}^k)) \tag{14}$$

where $\chi = 2 \left(\left| 2 - \varphi - \sqrt{\varphi^2 - 4\varphi} \right| \right)^{-1}$, $\varphi = c_1 + c_2$, and $\varphi > 4$. Common values of acceleration coefficients are $c_1 = c_2 = 2.05$, thus $\chi = 0.7298$. CPSO not only induces particles to convergence on local optima, but also prevents swarm explosion, which is a common problem with traditional PSO algorithms [19]. In this study, this version of the PSO will be used since its stability and convergence speed are better than those of the classic PSO. The algorithm was executed in MATLAB environment. Initial values of particles and their velocities were obtained drawing random numbers within the range of each dimension [20], i.e.

$$\begin{aligned}
 x_{ij}^1 &= x_{LB,j} + R.(x_{UB,j} - x_{LB,j}), \\
 v_{ij}^1 &= x_{LB,j} + R.(x_{UB,j} - x_{LB,j})
 \end{aligned}
 \tag{15}$$

where $x_{LB,j}$ and $x_{UB,j}$ are, respectively, lower and upper boundary values of the j th dimension, and $R \in$

$U(0,1)$. Besides, if a particle moves beyond ranges, then it is bounced back to the search space in the following way:

$$\begin{aligned}
 x_{ij}^k &= x_{UB,j} - R.(x_{ij}^k - x_{UB,j}), & \text{if } x_{ij}^k > x_{UB,j} \\
 x_{ij}^k &= x_{LB,j} + R.(x_{LB,j} - x_{ij}^k), & \text{if } x_{ij}^k < x_{LB,j}
 \end{aligned}
 \tag{16}$$

3. NUMERICAL SOLUTION

3.1. Case Studies

Using the same beam and vehicle parameters, the damage scenarios in Table 1 are considered. Road surface roughness is excluded for now, since its effect will be dealt with in the next section. To simulate the real situation, certain amount of noise is added to the reference data as follows [6]

$$\bar{y}(z,t)_{\text{noisy}} = \bar{y}(z,t)_{\text{calc}} + N_p \cdot G \cdot \sigma \quad (17)$$

where $\bar{y}(z,t)_{\text{calc}}$ is the calculated response of point z of the damaged beam (see Eq.(10)), N_p is the noise percentage, G is Gaussian distribution with zero mean and unit standard deviation, σ is the standard deviation of $\bar{y}(z,t)_{\text{calc}}$. Clearly, the first damage case in Table 1 is simpler than the second, since the dimension of the problem and the amount of noise are lower whereas crack size is bigger in the first case than those of the other case. Besides, the moving vehicle's speed is lower in the first case. This is significant, as the wavelet

transform methods lose sensitivity to damage at higher moving load/vehicle speeds [6-8,10]. Thus, damage identification ability at higher speeds can be deemed as an advantage of the method. Swarm size (N) and maximum iteration number were determined by experience as $N=20$ and $K_{\text{max}}=30$ for Case 1. These are selected as $N=30$ and $K_{\text{max}}=60$ for Case 2, considering the dimension of the problem. Algorithm was run ten times for each case due to its stochasticity [13], and the mean values of results are given in Table 2. Additionally, iterative variation of the objective function is given in Fig. 3 for the best runs, i.e. the run having minimum objective function value. From Table 2 it is clear that the proposed method can successfully locate damage locations and estimate crack sizes for Case 1. Crack locations and depths are determined with the relative errors smaller than 1%. However, the error in the value of objective function is remarkable, which is because of the sensitivity of the objective function to the small changes in location and depth variables. On the other hand, although the errors in the results are higher for Case 2, it is seen most of the parameters are determined with the error smaller than 10%.

Table 1. Damage scenarios.

Case	Crack Parameters	V_p (m/s)	N_p (%)
1	$\bar{z}_1 = 0.5, \bar{h}_1 = 0.3$	5	1
2	$\bar{z}_1 = 0.3, \bar{h}_1 = 0.1$ $\bar{z}_2 = 0.5, \bar{h}_2 = 0.1$ $\bar{z}_3 = 0.7, \bar{h}_3 = 0.1$	20	3

Table 2. Simulation results of the cases in Table 1.

Case		\bar{z}_1	\bar{z}_2	\bar{z}_3	\bar{h}_1	\bar{h}_2	\bar{h}_3	f^*
1	Exact	0.5000	---	---	0.3000	---	---	0.0375
	Predicted	0.4995	---	---	0.3002	---	---	0.0418
	ε	0.1	---	---	0.07	---	---	11.5
2	Exact	0.3000	0.5000	0.7000	0.1000	0.1000	0.1000	0.053
	Predicted	0.26	0.4949	0.7428	0.095	0.1183	0.0968	0.0536
	ε	11.9	1.1	6.1	5.01	18.3	3.15	0.56

*: See Eq. (10), $\varepsilon := 100 \times |E - Pr| / E$, E: Exact, Pr: Predicted

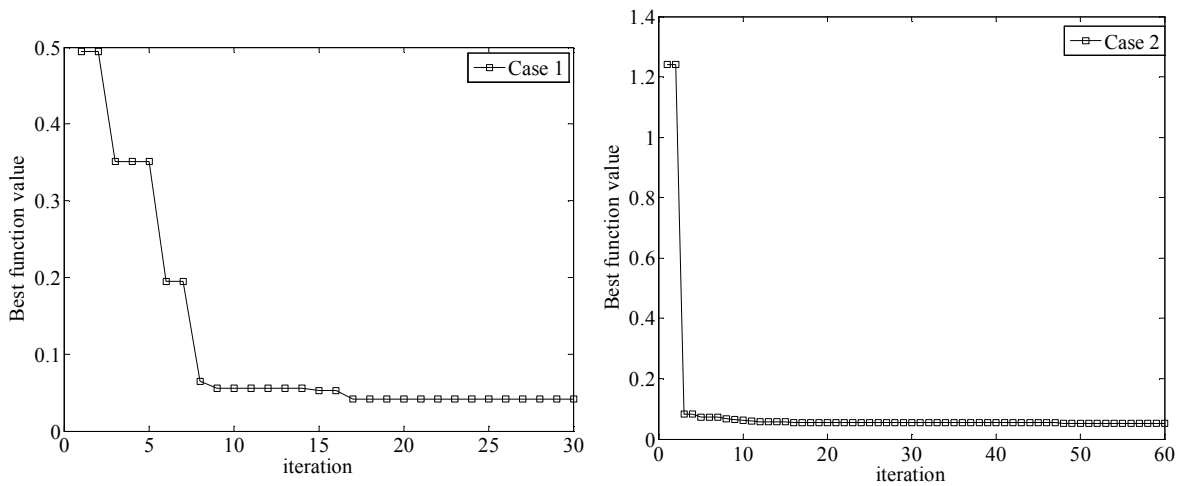


Figure 3. Variation of objective function with iteration.

3.2. Effect of Road Surface Roughness

As indicated previously road surface roughness affects the variation of dynamic response (see Fig.2). Since roughness function is random, each measurement produces different deflection profile [17], i.e. \bar{y} in Eq.(10). To indicate this let's consider Case 2 in Table 1. Fig. 4 illustrates five deflection time histories of the midspan with $S_d(f_0)=16 \times 10^{-6}$ for this case. It is seen that each curve is different from the others due to stochasticity of the roughness function. Thus, the proposed method cannot be implemented with single deflection profile recorded from measurement point. Fortunately, the roughness function in Eq.(4) has Gaussian distribution, i.e. the stochastic process composed of many roughness functions has the probability density function which is well correlated with that of the Gaussian process [17]. Thus, if deflection time history of a point on the damaged beam is measured many times and averaged, then the mean value of the deflections becomes closer to the one obtained by ignoring the roughness and noise, i.e. the

function y in Eq.(10). This is demonstrated in Fig. 5 for the same case. The figure implies that the more the number of averages, the better the correlation between the computed and average deflections, i.e. y and \bar{y} . It is obvious that not only the average curve is well correlated with the reference one but also noise is eliminated to a great extent by averaging. Employing the averages of measured displacements the results in Table 3 are obtained. The numbers in parentheses indicate the number of averages. That is, if the average of 50 deflection time histories from a measurement point is employed, then the value of objective function is 0.031 and the crack parameters are as shown in the relevant line of the table. It is clear that more average means better results. In the case of 50 average the number of variables with relative error bigger than 10% is 4 whereas it is 1 for the case of 100 average. In the case of 200 average the errors are lower than the previous. Hence, using the averages of many deflection profiles instead of one obtained by single measurement promotes the applicability of the method and enhances the accuracy of predicted results.

Table 3. Simulation results of Case 2 in Table 1 including road surface roughness.

	\bar{z}_1	\bar{z}_2	\bar{z}_3	\bar{h}_1	\bar{h}_2	\bar{h}_3	f^*
E	0.3000	0.5000	0.7000	0.1000	0.1000	0.1000	0.0288
Pr (50Av.)	0.2655	0.5449	0.8025	0.0989	0.1200	0.0793	0.0310
ε	11.5	8.9	14.6	1.08	20	20.1	7.34
E	0.3000	0.5000	0.7000	0.1000	0.1000	0.1000	0.0205
Pr (100Av.)	0.3287	0.5471	0.8114	0.1062	0.1047	0.1061	0.0214
ε	9.6	9.4	16	6.1	4.7	6.1	4.4
E	0.3000	0.5000	0.7000	0.1000	0.1000	0.1000	0.0111
Pr (200Av.)	0.2739	0.5028	0.7262	0.1033	0.1104	0.1007	0.0080
ε	8.7	0.6	3.7	3.3	10.4	0.7	27

*: Eq. (10), $\varepsilon=100x|E-Pr|/E$, E: Exact, Pr: Predicted.

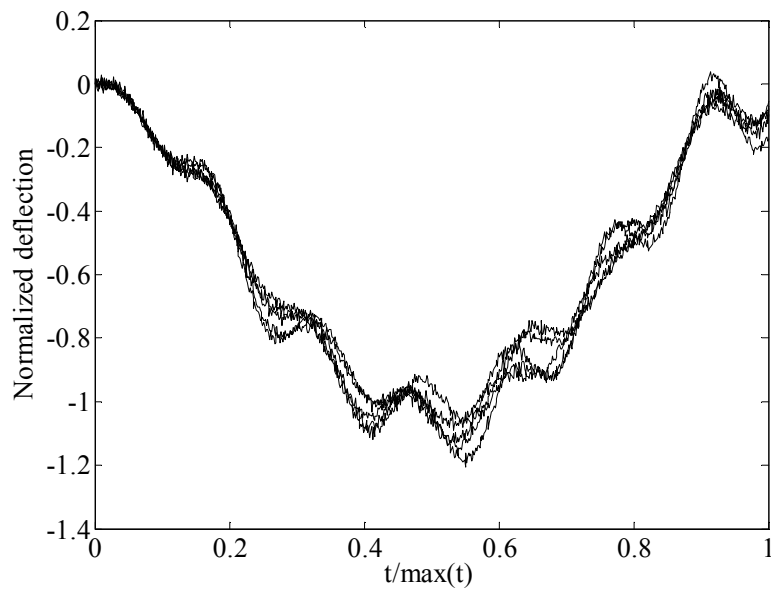


Figure 4. Midspan deflections of the beam corresponding to five different roughness profiles.

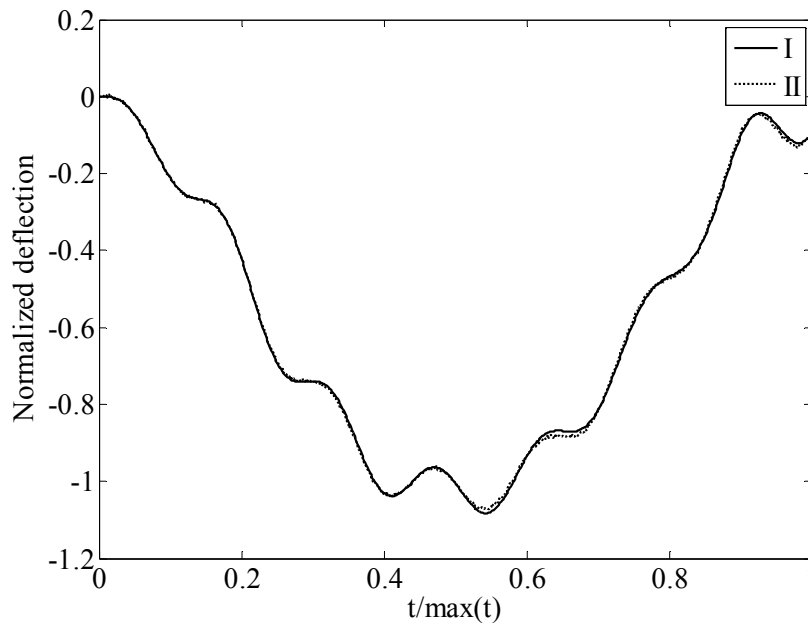


Figure 5. (a): Comparison of midspan deflections for Case 2 in Table 1 (I: No noise and roughness, II: Average of 20 deflection curves including noise and roughness).

4. CONCLUSIONS

In this study, a new crack identification method for beam type structures carrying moving vehicle is proposed. Damage detection was formulated as an optimization problem using difference of measured time dependent deflections of the damaged beam and those computed by the mathematical model of the structure. Then, this is solved by a robust evolutionary algorithm, i.e. the particle swarm optimization, for crack locations and depth. Both road surface roughness and measurement noise are considered. It was demonstrated that crack size of 0.1 can be determined by the proposed approach with relative error nearly 10%. The drawback of the method is that it is difficult to obtain by a single measurement the reference data well-correlated with the one computed by the mathematical model of the structure. This is because of the random nature of road surface roughness, which gives rise to different deflection profile at every measurement. However, average of multiple measurements is well-correlated with the one computed by the mathematical model. Thus, the proposed method can be implemented provided the average of multiple measurements is employed as reference. Future works are planned to consider the opening and closing of crack during the simulation, and test the method with real data.

REFERENCES

- [1] Frýba, L., 'Vibration of Solids and Structures Under Moving Loads', *Telford*, London, (1999).
- [2] Mahmoud, M.A., "Effect of cracks on the dynamic response of a simple beam subject to a moving load", *Proceedings of the Institution of Mechanical Engineers*, 215: 207-215, (2001).
- [3] Bilello, C. and Bergman, L.A., "Vibration of damaged beam under a moving mass: theory and experimental validation", *Journal of Sound and Vibration*, 274: 567-582, (2004).
- [4] Law, S.S. and Zhu, X.Q., "Dynamic behaviour of damaged concrete bridge structures under moving vehicular loads", *Engineering Structures*, 26: 1279-1293, (2004).
- [5] Ariaei, A., Ziaei-Rad, S., and Ghayour, M., "Vibration analysis of beams with open and breathing cracks subjected to moving masses", *Journal of Sound and Vibration*, 326: 709-724, (2009).
- [6] Zhu, X.Q., Law, S.S., "Wavelet-based crack identification of bridge beam from operational deflection time history", *International Journal of Solids and Structures*, 43: 2299-2317, (2006).
- [7] Hester, D., Gonzalez, A., "A wavelet-based damage detection algorithm based on bridge acceleration response to a vehicle", *Mechanical Systems and Signal Processing*, (2011), doi:10.1016/j.ymssp.2011.06.007.
- [8] Nguyen, K.V., Tran, H.T., "Multi-cracks detection of a beam-like structure based on the on-vehicle vibration signal and wavelet analysis", *Journal of Sound and Vibration*, 329: 4455-4465, (2010).

- [9] Khorram, A., Bakhtiari-Nejad, F., and Rezaeian, M., "Comparison studies between two wavelet based crack detection methods of a beam subjected to a moving load", *International Journal of Engineering Science*, 51: 204-215, (2012).
- [10] Gökdağ, H., "Wavelet-based damage detection method for a beam-type structure carrying moving mass", *Structural Engineering and Mechanics*, 38(1): 81-97, (2011).
- [11] Buezas, F.S., Rosales, M.B., Filipich, C.P., "Damage detection with genetic algorithms taking into account a crack contact model" *Engineering Fracture Mechanics*, 78(4): 695-712, (2011).
- [12] Begambre, O., and Laier, J.E., "A hybrid particle swarm optimization – simplex algorithm (PSOS) for structural damage identification", *Advances in Engineering Software*, 40: 883-891, (2009).
- [13] Moradi, S., Razi, P. and Fatahi, L., "On the application of bees algorithm to the problem of crack detection", *Computers and Structures*, 89: 2169-2175, (2011).
- [14] Seyedpoor, S.M., "A two stage method for structural damage detection using a modal strain energy based index and particle swarm optimization", *International Journal of Non-Linear Mechanics*, 47: 1-8, (2012).
- [15] Kennedy, J., Eberhart, R., "Particle swarm optimization", *Proceedings of the 4th IEEE International Conference on Neural Networks*, 4: 1942-1948, (1995).
- [16] Parsopoulos, K.E., Vrahatis, M.N., Particle swarm optimization and intelligence: Advances and Applications. IGI Global, Hershey PA, (2010).
- [17] Wu, S.Q., Law, S.S., "Vehicle axle load identification on bridge deck with irregular road surface profile", *Engineering Structures*, 33: 591-601, (2011).
- [18] Clough, R.W., Penzien, J., Dynamics of Structures. Computers & Structures, Inc., Berkeley, CA, (1995).
- [19] Clerc, M., Kennedy, J., "The particle swarm-explosion, stability, and convergence in a multidimensional complex space", *IEEE Transactions on Evolutionary Computation* 6(1): 58-73, (2002).
- [20] Trelea, I.C., "The particle swarm optimization algorithm: convergence analysis and parameter selection", *Information Processing Letters*, 85: 317-325, (2003).